JOURNAL OF WATER AND LAND DEVELOPMENT
e-ISSN 2083-4535
Polish Academy of Sciences (PAN) Institute of Technology and Life Sciences – National Research Institute (ITP – PIB)

JOURNAL OF WATER AND LAND DEVELOPMENT
DOI: 10.24425/jwld.2026.157832
2026, No. 68 (I–III): 158–170

Modelling future landscape fragmentation through integrated simulation and metrics-based analysis in Bila Watershed, Indonesia

Reza Asra[1), 2)], Ahmad Munir*[1)], Hazairin Zubair[1)], Mahmud Achmad[1)]

[1)] Hasanuddin University, Doctoral Program, Department of Agricultural Science, Jalan Perintis Kemerdekaan, KM. 10, Makassar, South Sulawesi, 90245, Indonesia

[2)] Universitas Muhammadiyah Sidenreng Rappang, Department of Agrotechnology, Jalan Angkatan, 45 No. 1A, Lautang Salo Rappang, Sidenreng Rappang, South Sulawesi, 91651, Indonesia

* Corresponding author

RECEIVED 09.08.2025 ACCEPTED 31.10.2025 AVAILABLE ONLINE 18.03.2026

HIGHLIGHTS

- Integrates a CA–ANN model with landscape metrics to assess fragmentation patterns.
- Projects 2030 and 2036 LULC in a tropical watershed of Indonesia.
- Forest cover declined by 9.14%, while NP and SHDI showed substantial increases.
- The CA–ANN model achieved high predictive accuracy ($k_{overall}$ = 0.94; *OA* = 96.19%).
- Supports SDG 15 and informs landscape planning in data-scarce tropical regions.

Abstract: Land use and land cover (LULC) changes are significant factors driving ecological shifts and landscape fragmentation. However, most predictive frameworks rarely integrate spatial simulations with structural landscape interpretations, particularly in tropical watersheds. This study presents an integrated cellular automata–artificial neural network (CA–ANN) framework coupled with landscape metrics to predict future fragmentation in the Bila Watershed, South Sulawesi, Indonesia. Multi-temporal Landsat data (2012, 2018, 2024) were classified, and future scenarios for 2030 and 2036 simulated. Five landscape metrics were computed, including number of patches (*NP*), largest patch index (*LPI*), edge density (*ED*), proportion of landscape (*PLAND*), and Shannon's diversity index (*SHDI*). The CA–ANN model achieved high predictive performance (overall kappa ($k_{overall}$) = 0.94, overall accuracy (*OA*) = 96.19%). From 2012 to 2036, forest cover (*PLAND*) declined (from 56 to 51%), the landscape's *LPI* decreased (from 54.93 to 50.48), and *SHDI* increased (from 1.241 to 1.323), indicating growing heterogeneity and declining core forest dominance. Concurrently, *NP* (from 295 to 552) and *ED* (from 0.0019 to 0.0033 m·ha^{-1}) for dryland agriculture surged, indicating intensified patch proliferation in agricultural zones. The cumulative conversion of 5,690 ha of forest and shrubland into agriculture, mainly in the upper and accessible terrains, emerged as the dominant structural driver. By linking predictive accuracy with ecological structure, this framework enhances LULC modelling for landscape planning, risk assessment, and sustainable watershed management. Fully reproducible with open-source Geographic Information Systems (GIS), the approach supports Sustainable Development Goal 15 ("Life on land").

Keywords: artificial neural network (ANN), cellular automata (CA), land use and land cover (LULC), patch analysis, simulation framework, spatial modelling, tropical watershed

INTRODUCTION

Land use and land cover (LULC) change is widely recognised as one of a principal driver of environmental degradation, threatening biodiversity, disrupting ecosystem services, altering climate regulation, and undermining global food security (Sharma *et al.*, 2022; Alemayehu *et al.*, 2024). From 2000 to 2020, global forest cover declined by more than 178 mln ha, an area comparable to Libya, mainly because of agricultural expansion and infrastructure development (FAO, 2020). These impacts are particularly severe in tropical regions, which contain the planet's richest biodiversity, where more than 80% of documented species extinctions have been attributed to land-use conversion, especially agricultural encroachment (Cabernard *et al.*, 2024).

One of the most critical, yet often overlooked, consequences of LULC change is landscape fragmentation, which currently affects more than 60% of global watershed systems (Alaei *et al.*, 2022). Fragmentation disrupts spatial connectivity, reduces patch size, and isolates habitats, thereby weakening ecological integrity and microclimatic stability (Thomas *et al.*, 2020). In Southeast Asia, annual deforestation exceeds 1.2 mln ha and is largely driven by smallholder agriculture, plantation expansion, and peri-urban development (Hansen *et al.*, 2020). In Indonesia, almost half of the forests outside protected areas have been fragmented, causing notable hydrological and ecological impacts (Harrison *et al.*, 2019; Dharmawan *et al.*, 2023). The Bila Watershed in South Sulawesi exemplifies this pattern, where rapid land changes endanger landscape stability, sediment retention, and downstream agroecosystem resilience (Asra *et al.*, 2020; Abdullah *et al.*, 2022).

To anticipate and manage these transformations, spatially explicit LULC modelling has become an essential analytical tool for sustainable land management and regional planning (Moreira *et al.*, 2024). Among the available approaches, the hybrid cellular automata-artificial neural network (CA–ANN) model has gained attention for its ability to simulate nonlinear transitions and spatial dependencies in complex landscapes (Baig *et al.*, 2022; Islam *et al.*, 2023). The integration of this model into open-source geographic information system (GIS) platforms, such as the MOLUSCE plugin in quantum geographic information system (QGIS), has further increased its accessibility and applicability to a wide range of land-change scenarios (Skilodimou *et al.*, 2023; Din and Yamamoto, 2024). Despite these advances, most previous studies have focused on model calibration and spatial accuracy, with limited attention to the ecological structure or functional consequences of land-use transitions. For example, Xu *et al.* (2021) and Liang *et al.* (2021) refined driver selection to improve model precision but did not explicitly link their predictive outputs to quantitative indicators of landscape fragmentation. Several recent studies have incorporated landscape metrics into post-simulation analyses (Talukdar *et al.*, 2021; Matyukira and Mhangara, 2023; Rojas Celis *et al.*, 2025); however, the integration between predictive modelling and structural interpretation remains weak, particularly within tropical watershed systems, where data scarcity and complex land–human interactions reduce model interpretability.

This study addresses methodological and contextual gap by developing an integrated CA–ANN–metrics framework to simulate and interpret future landscape fragmentation in the Bila Watershed, South Sulawesi, Indonesia. This approach links predictive accuracy with ecological structure by quantifying fragmentation dynamics through five core metrics: number of patches, largest patch index, edge density, proportion of landscape, and Shannon's diversity index, which collectively represent the most essential landscape composition (Lin *et al.*, 2024; Zhu *et al.*, 2021). Unlike empirical or rule-based models such as CA-Markov or conversion of land use and its effects at small regional extent (CLUE-S), the CA–ANN algorithm employs a data-driven learning process that can capture complex spatial dependencies in heterogeneous tropical environments (Fetene *et al.*, 2023). By integrating simulation and landscape metrics within an entirely open-source QGIS 3.34 environment, this study offers methodological advancements and applied insights. The methodological contribution shows a reproducible framework linking spatial modelling with landscape metrics, while the applied part offers evidence-based insights into fragmentation in a data-scarce tropical watershed. Through this integration, the study strengthens the interpretive value of land-use modelling and contributes to sustainable landscape management aligned with Sustainable Development Goal 15 ("Life on land").

MATERIALS AND METHODS

STUDY AREA

The Bila Watershed is a critical upstream catchment located in South Sulawesi, Indonesia, and serves as the primary source of irrigation water for agricultural activities in the region. The watershed drains into Lake Tempe, one of the most essential hydrological systems in southern Sulawesi, supporting extensive downstream rice cultivation and agroecosystems. Covering approximately 54,511.09 ha, the Bila catchment extends across three administrative districts (Enrekang, Sidenreng Rappang and Wajo) in South Sulawesi Province. As a headwater region, it plays a key role in regulating water availability, sediment transport, and landscape stability. Geographically, the catchment lies between 119°55'0"–120°10'0" E and 3°33'20"–3°53'20" S. The location of the watershed is illustrated in Figure 1.

STUDY MATERIALS

This study employed multi-temporal Landsat imagery (2012, 2018, and 2024; path/row 114/62 and 114/63) with less than 10% cloud cover, acquired from the USGS Earth Explorer (https://earthexplorer.usgs.gov/). All scenes were pre-processed through georeferencing, mosaicking, subsetting, and reprojection to the WGS 1984 UTM Zone 50S coordinate system. Topographic data were derived from the 30 m Shuttle Radar Topography Mission (SRTM) Digital Elevation Model (https://srtm.csi.cgiar.org/), while infrastructure and hydrological features were digitised from the Indonesian Earth Map (RBI 1:50,000) provided by the Indonesian Geospatial Information Agency (BIG) (https://tanahair.indonesia.go.id/portal-web). These datasets were cross-verified against the 2024 Landsat classification results and field checks to ensure spatial accuracy and thematic consistency. All datasets are publicly accessible and were processed entirely within an open-source GIS environment (QGIS 3.34), ensuring methodological transparency and reproducibility.

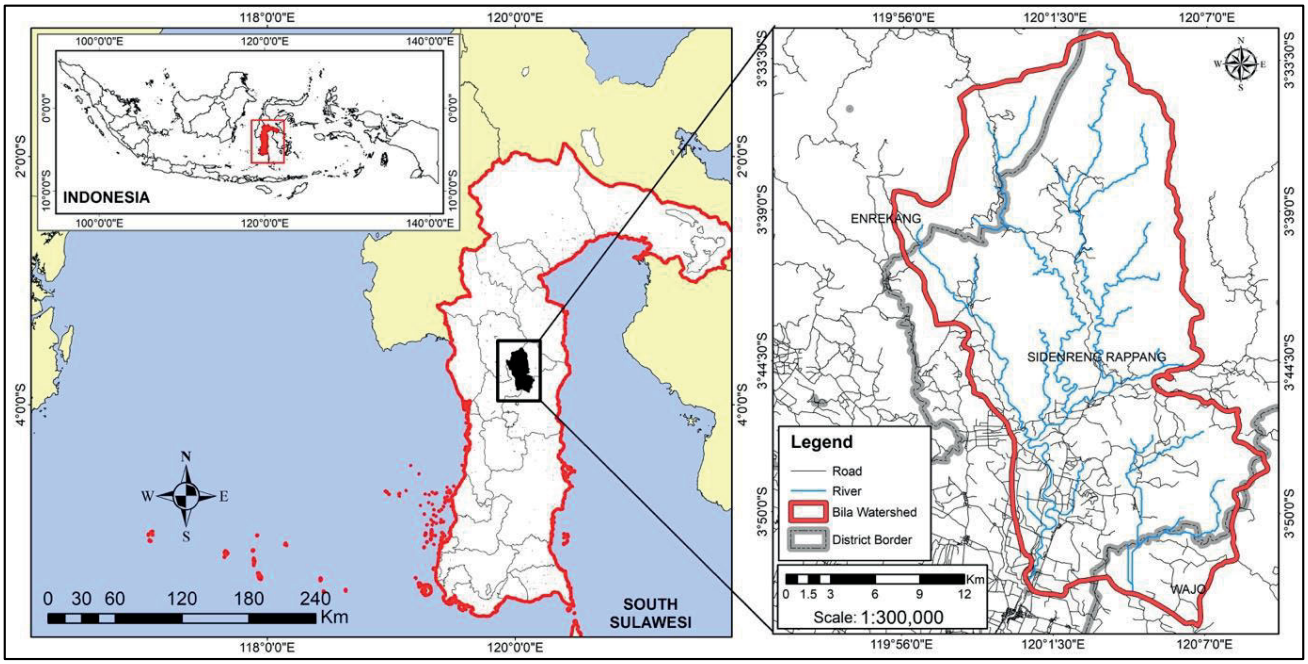

Fig. 1. Location of the Bila Watershed, Indonesia; source: own elaboration

Five spatial drivers were selected to represent the key determinants of land-use processes: slope, distance to road (d_{road}), distance to settlement (d_{settl}), distance to public facilities (d_{pf}), and distance to river (d_{river}). These factors are widely recognised as determinants of land suitability, accessibility, and development potential (Abbas *et al.*, 2021; Lukas *et al.*, 2023). Although no explicit socioeconomic variables were included due to data availability and spatial resolution constraints, the selected spatial drivers implicitly captured socioeconomic and human accessibility effects. This assumption is consistent with recent CA–ANN studies in data-scarce tropical regions, where accessibility-based variables are commonly used as reliable spatial proxies for socioeconomic drivers (Baig *et al.*, 2022; Din and Yamamoto, 2024; Mishra *et al.*, 2024).

The slope variable was derived from the DEM, whereas the distance variables were computed using the Euclidean distance method, which calculates straight-line proximity and has proven effective in the spatial modelling of LULC transitions (Gharaibeh *et al.*, 2020). The Euclidean distance is defined as:

$$d_{(a,b)} = \sqrt{\sum_{i=1}^{n} (a_i - b_i)^2} \quad (1)$$

where: $d_{(a,b)}$ = Euclidean distance between two points a and b in the n-dimensional space (Diep *et al.*, 2025).

STUDY METHODS

The methodological framework of this study includes three stages: (i) LULC classification and accuracy assessment, (ii) CA–ANN modelling and validation, and (iii) computation of landscape metrics.

Land use and land cover classification and accuracy assessment

Maps of LULC for 2012, 2018, and 2024 were generated using pixel-based supervised classification with the Semi-Automatic Classification Plugin (SCP) in QGIS (Congedo, 2021). The maximum likelihood algorithm was selected due to its high accuracy for multispectral datasets (El Moussaoui *et al.*, 2025). A total of 120 training samples per year were assigned across six LULC classes: forest, shrubland, dryland agriculture, wetland agriculture, built-up area, and water bodies, based on the Indonesian National Standard SNI 7645:2010 (BSN, 2010; BSN, 2014). Spectral enhancement was applied to improve class separability (Toosi *et al.*, 2020).

Classification accuracy was assessed using the AcATAMa plugin in QGIS, which generates confusion matrices and computes standard accuracy metrics, including overall accuracy (OA) and Kappa coefficient (κ) (Sujarwo *et al.*, 2023), as follows:

$$OA = \frac{N_{correct}}{N_{total}} 100 \quad (2)$$

$$\kappa = \frac{N \sum_{i=1}^{n} a_{i,i} - \sum_{i=1}^{n} (T_i F_i)}{N^2 - \sum_{i=1}^{n} (T_i F_i)} \quad (3)$$

where: $N_{correct}$ = number of correctly classified pixels, N_{total} = total number of reference pixels (samples), N = total number of samples, $a_{i,i}$ = number of correctly classified pixels in class i, and T_i and F_i = row and column totals, respectively; $\kappa > 0.90$ indicates a very high agreement (Blissag *et al.*, 2024).

Cellular automata–artificial neural network modelling and validation

Projections of LULC for 2030 and 2036 were conducted using the CA–ANN model embedded in the Modules for Land Use Change Evaluation (MOLUSCE) plugin in QGIS. The workflow included spatial variable preparation, correlation analysis, transition probability modelling, ANN training, and CA-based simulation (Muhammad *et al.*, 2022). Datasets from 2012, 2018, and 2024 were used as inputs. During calibration, the model learned transition relationships from the 2012–2018 data through an

iterative training process. All five spatial drivers (slope, d_{road}, d_{settl}, d_{pf}, and d_{river}) were resampled to a 30 m resolution and aligned to a uniform spatial grid.

The ANN component used a feedforward multilayer perceptron (MLP) trained by backpropagation with a learning rate of 0.001, momentum of 0.001, 100 iterations, and ten hidden neurons (Baig *et al*., 2022; Kamaraj and Rangarajan, 2022). The model adjusts neuron connection weights to minimise the prediction errors between modelled and observed transitions (Lukas *et al*., 2023). Historical change detection (2012–2018) was used to build a transition probability matrix, from which MOLUSCE automatically extracted training samples representing changed and unchanged pixels. Upon convergence, the ANN produced transition potential maps indicating the likelihood of pixel-level transitions for each LULC class (Belay *et al*., 2024). The CA component then spatially allocated transitions using a 3×3 Moore neighbourhood to maintain spatial contiguity and local neighbourhood effects (Xu *et al*., 2021). Model calibration was verified by assessing the convergence of the neural network learning curve (NNLC) and consistency between training and validation errors (Hussain *et al*., 2025).

The model performance was validated by simulating the 2024 LULC and comparing it to the observed 2024 map using three kappa-based validation metrics: overall, location, and histogram (Uddin *et al*., 2023):

$$k_{\text{overall}} = \frac{(\sum_{i=1}^{c} P_{ij}) - (\sum_{i=1}^{c} P_{it}P_{tj})}{1 - (\sum_{i=1}^{c} P_{it}P_{tj})} \tag{4}$$

$$k_{\text{local}} = \frac{(\sum_{i=1}^{c} P_{ij}) - (\sum_{i=1}^{c} P_{it}P_{tj})}{\min(P_{it}P_{tj}) - (\sum_{i=1}^{c} P_{it}P_{tj})} \tag{5}$$

$$k_{\text{histogram}} = \frac{\min(P_{it}P_{tj}) - (\sum_{i=1}^{c} P_{it}P_{tj})}{1 - (\sum_{i=1}^{c} P_{it}P_{tj})} \tag{6}$$

where: P_{ij} = proportion of pixels in the i,j^{th} cell of the confusion matrix, P_{it} and P_t = row and column marginal probabilities, respectively, and c = number of LULC classes.

Once satisfactory validation was achieved, the model was applied under a business-as-usual (BAU) scenario to project future conditions. Two independent simulations were conducted: (i) 2030, based on 2018–2024 data, and (ii) 2036, based on 2012–2024. Both simulations used an identical ANN configuration. The resulting transition potential surfaces formed the foundation for analysing land-use dynamics and quantifying landscape fragmentation metrics in subsequent analyses.

Landscape metric computation

To quantify spatial fragmentation and landscape structure, five key landscape metrics were computed: number of patches (*NP*), largest patch index (*LPI*), edge density (*ED*), proportion of landscape (*PLAND*), and Shannon's diversity index (*SHDI*). These indices collectively represent the most essential and non-redundant dimensions of landscape composition and configuration, providing a balanced description of fragmentation intensity, patch dominance, edge complexity, and class-level diversity (Zhu *et al*., 2021; Lin *et al*., 2024). Specifically, *NP* and *LPI* describe landscape composition and dominance, *ED* measures boundary complexity, *PLAND* quantifies class-level extent, and *SHDI* represents the overall heterogeneity. The integration of composition- and configuration-based metrics provides robust indicators of ecological fragmentation and spatial resilience, particularly in dynamic tropical systems (Li *et al*., 2025; Zhang *et al*., 2025).

All metrics were calculated using the landscape ecology statistics (LecoS) plugin in QGIS, which automates patch- and class-level calculations based on the FRAGSTATS algorithm (Huang *et al*., 2024). The outputs were cross-checked using raster–vector overlays and benchmarked against SAGA GIS–based calculations for consistency (García-Álvarez and Paegelow, 2022; Huang *et al*., 2024). The formulas for each metric are as follows:

$$NP = n \tag{7}$$

$$LPI = \left(\frac{\max(a_{ij})}{A}\right)100 \tag{8}$$

$$ED = \frac{E}{A}10^4 \tag{9}$$

$$PLAND = \left(\frac{\sum a_{ij}}{A}\right)100 \tag{10}$$

$$SHDI = -\sum_{i=1}^{m}(p_i \cdot \ln p_i) \tag{11}$$

where: n = number of patches of a given class, a_{ij} = area of patch j in class i, A = total landscape area (ha), E = total edge length (m), p_i = proportion of landscape occupied by class i, and m = number of classes (Maity and Mishra, 2024).

RESULTS AND DISCUSSION

LULC CHANGE ANALYSIS AND EVALUATION

The accuracy assessment of the multitemporal LULC maps for 2012, 2018, and 2024 confirmed high classification reliability, with overall accuracies of 92.78%, 93.89%, and 93.33%, respectively, and kappa coefficients (κ) ranging from 0.91 to 0.92. These values indicate a strong agreement between the classified and reference data. The slightly lower accuracy in 2012 was attributed to the scan-line corrector malfunction of Landsat-7 ETM+, which reduced the radiometric quality (Adıyaman *et al*., 2025). In contrast, the superior spectral fidelity of Landsat-8 OLI/TIRS in later years improved class separability and mapping consistency (Mancino *et al*., 2020; Perez and Vitale, 2023). According to Pandey *et al*. (2023), consistently high kappa coefficient (κ) values validate the robustness of the classification scheme, indicating that observed spatial changes reflect actual land transformations.

From 2012 to 2024, the Bila Watershed experienced marked restructuring of LULC composition. Forests remained the dominant class but declined from 30,413.49 ha (55.79%) to 29,253 ha (53.66%), representing a net loss of (−3.81%). Shrubland declined even more sharply (−16.53%), primarily due to conversion to agricultural land. Conversely, dryland agriculture expanded from 7,565.96 to 9,039.93 ha (+19.48%), and wetland agriculture grew from 4,859.08 to 6,180.67 ha (+27.19%).

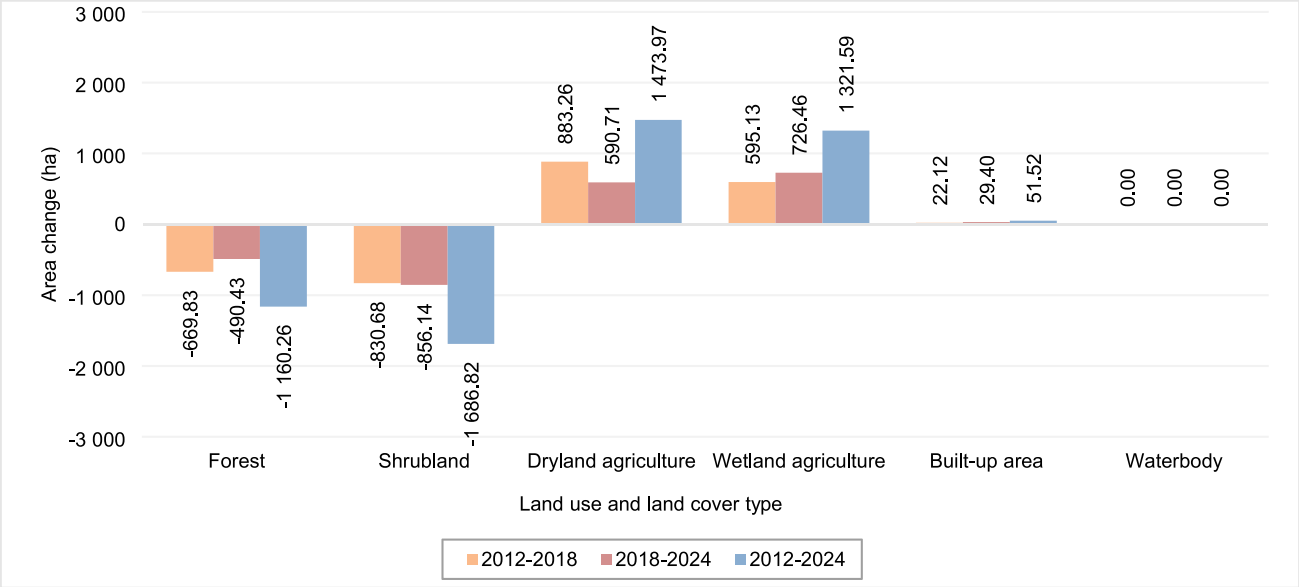

Fig. 2. The net land use and land cover (LULC) area changes in the Bila Watershed from 2012 to 2024; source: own study

Built-up areas increased modestly from 344.16 to 395.68 ha (+14.97%), reflecting gradual peri-urban development, whereas the area of water bodies remained relatively stable.

As shown in Figure 2, forest and shrubland losses closely match the gain in agricultural land (+2,795.56 ha), indicating a one-to-one replacement due to increased cultivation in vegetated areas. The substitution of natural vegetation with cropland represents the dominant process shaping the evolving structure of the watershed. According to Hansen *et al.* (2020) and Santoro *et al.* (2023), this pattern aligns with broader land-use transitions documented across Southeast Asian watersheds, where the expansion of smallholder and commercial agriculture has become the principal driver of landscape changes.

The spatial distribution of these changes, as shown in Figure 3, indicates that forest edges near roads and rivers are especially vulnerable to encroachment, highlighting the shift from dense forest blocks to fragmented agro-forest areas mosaics. According to Christiawan and Nguyen (2024), these spatial configurations are consistent with the accessibility-driven land-use dynamics observed in other tropical watersheds. Simultaneously, the gradual expansion of agricultural areas and built-up land signals a shift in the functional use of land from primarily ecological to production-oriented landscapes. Such shifts are frequently accompanied by reduced hydrological regulation capacity, soil stability, and biodiversity connectivity (Liu *et al.*, 2022; Gong *et al.*, 2023). In the Bila Watershed, these changes foreshadow potential ecological stress, particularly in upland catchments, where vegetation cover plays a critical role in regulating runoff and sedimentation into the Lake Tempe. Overall, the LULC analysis for 2012–2024 demonstrated that the Bila Watershed is transitioning toward an agro-dominated mosaic landscape, characterised by a simultaneous contraction of natural vegetation and the expansion of human-managed land.

SIMULATION AND PROJECTION OF LULC CHANGE

Five spatial predictor variables were analysed using Pearson's correlation in the MOLUSCE plugin to model the correlation and potential transitions. The analysis revealed a strong positive association between d_{road} and d_{settl} (r = 0.872), indicating that built-up and agricultural expansion cluster around accessible transportation and settlement areas. Moderate correlations among the other variables suggest that topography and hydrology exert secondary, but spatially coherent, control over land transformation. The slope variable exhibited a positive relationship with d_{road} and d_{pf} but a weak negative correlation with d_{river}, reflecting the typical topographic gradient from highland forest areas to lowland agricultural plains. This relationships form a strong basis and align with the characteristics of the region to be included in the modelling. These relationships are illustrated in Figure 4.

Model calibration using the 2012–2018 LULC pair produced a simulated 2024 map that was validated against the field-verified 2024 classification. Validation metrics indicated excellent model performance ($k_{overall}$ = 0.94; $k_{location}$ = 0.98; $k_{histogram}$ = 0.96; OA = 96.19%), confirming the robustness of the CA–ANN model and its ability to replicate complex, nonlinear land-use dynamics in tropical watersheds (Abbas *et al.*, 2021; Blissag *et al.*, 2024). The neural network learning curve (NNLC) exhibited minimal divergence between training and validation (Fig. 5), indicating stable learning and generalisation (Din and Yamamoto, 2024).

From 2024 to 2036, the watershed is projected to experience intensified anthropogenic land use. The forest area declines from 29,252.99 to 27,632.12 ha (−1,620.87 ha; −5.54%), and the shrubland decreases from 8,514.37 to 7,448.64 ha (−1,065.73 ha; −12.52%). In contrast, dryland agriculture expands by 1,440.42 ha (+15.93%), wetland agriculture by 1,199.17 ha (+19.40%), and built-up areas by 47.01 ha (+11.88%), reflecting continued urban expansion. Water bodies remains relatively constant, reflecting a stable hydrological regime in the region. These transformations are shown in Figure 6.

From 2024 to 2036, forest-to-agriculture (1,543.74 ha) and shrubland-to-agriculture (1,203.4 ha) transitions are predicted to be the main land change drivers, accounting for over 63.5% transitions. Collectively, these transitions resulted in the loss of 2,747.14 ha of natural vegetation. Smaller but spatially significant transitions included an increase in the built-up area of

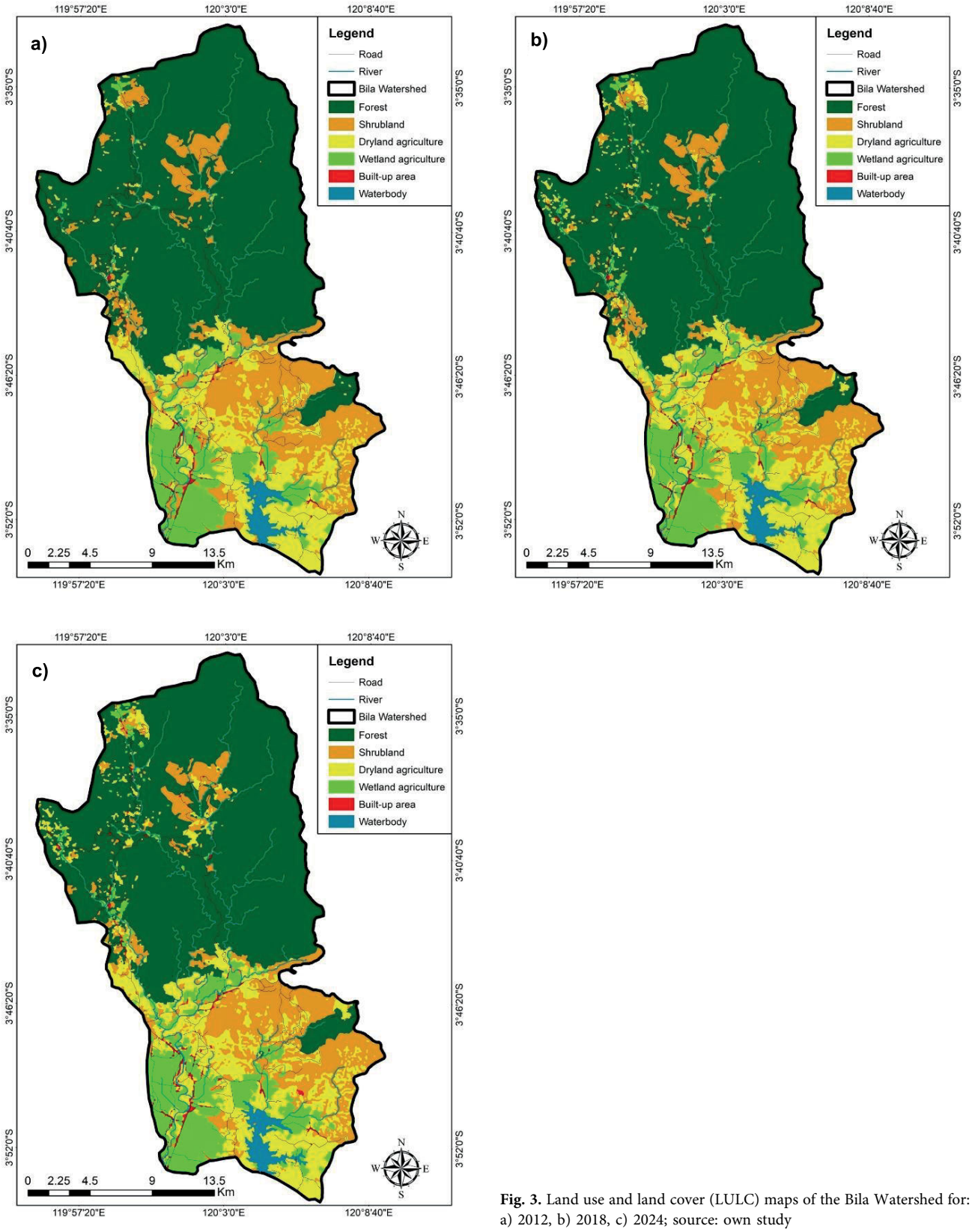

Fig. 3. Land use and land cover (LULC) maps of the Bila Watershed for: a) 2012, b) 2018, c) 2024; source: own study

47.01 ha, indicating incremental urbanisation along accessibility gradients. These conversion pathways highlight the dual processes of deforestation and agricultural intensification that characterise many tropical watersheds undergoing socioeconomic transitions (Mendoza-Ponce *et al.*, 2021; Biswas et *al.*, 2023).

As shown in Figure 7, the upper and middle catchments were identified as the most active transformation zones, particularly near the road networks and rivers. These areas showed proximity-driven land conversion, similar to tropical watersheds in Ethiopia and Indonesia (Leta *et al.*, 2021; Putra *et al.*, 2025), where agriculture followed accessibility, increasing slope instability and sedimenta-

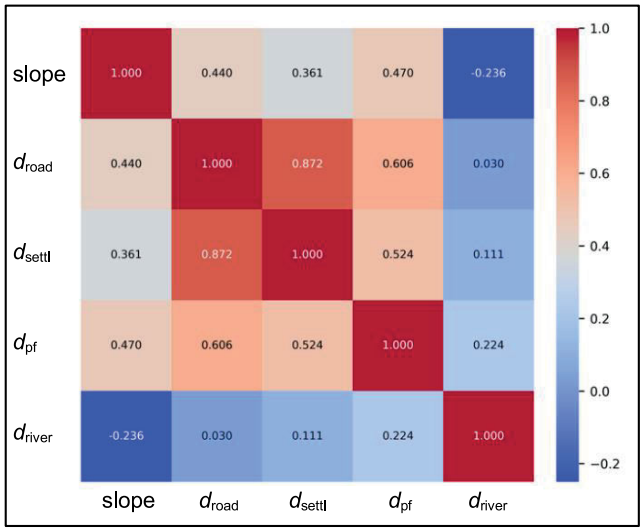

Fig. 4. The matrix correlation between spatial drivers using Pearson's method; d_{road} = distance to road, d_{settl} = distance to settlement, d_{pf} = distance to public facilities, d_{river} = distance to river; source: own study

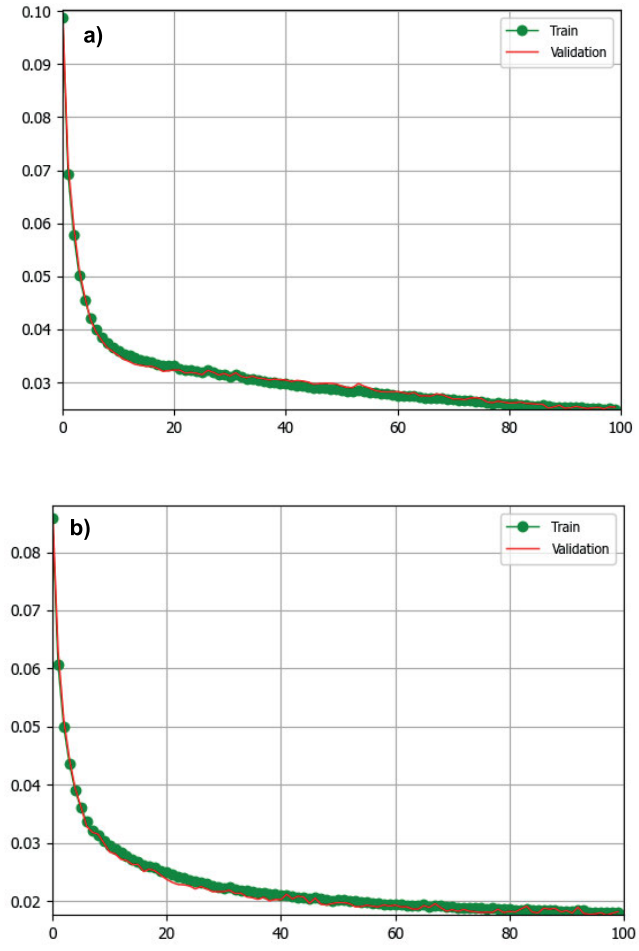

Fig. 5. Neural network learning curves (NNLC) for land use and land cover (LULC) projections in: a) 2030, b) 2036; source: own study

tion. The predicted LULC distributions for 2030 and 2036 reflect a landscape transitioning toward agricultural dominance, with ecological consequences, including reduced forest connectivity and decreased hydrological buffering capacity.

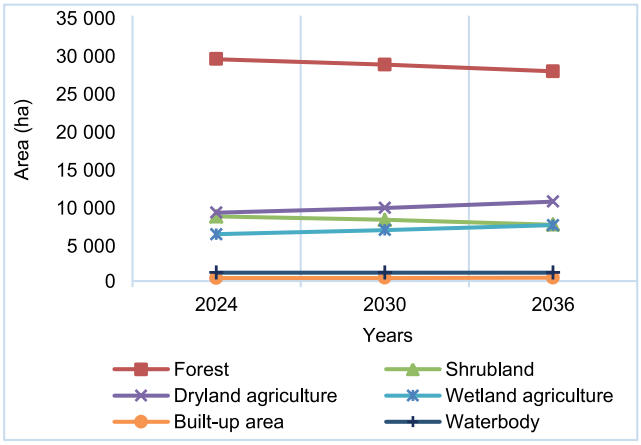

Fig. 6. Projected land use and land cover (LULC) changes in the Bila Watershed from 2024 to 2036 by category; source: own study

LANDSCAPE FRAGMENTATION

The spatiotemporal analysis of landscape structure from 2012 to 2036 showed a clear shift towards a more fragmented and diverse pattern in the Bila Watershed. Forest remained the dominant LULC type, but its extent declined from 30,413.25 ha (55.79%) to 27,632.12 ha (50.69%), reflecting a loss of 2,781.13 ha (–9.14%). Shrubland experienced an even greater relative decline, decreasing by 2,752.55 ha (–26.98%). The primary driver of this structural transformation was the conversion of natural vegetation into agricultural land, with a cumulative transition of 5,690.16 ha of forest and shrubland converted to dryland and wetland agriculture between 2012 and 2036. The most intensive transitions occurred during 2012–2018 (1,519.07 ha) and 2030–2036 (1,559.19 ha), corresponding to the early and late phases of agricultural expansion, respectively. Overall, these results indicate that fragmentation in the Bila landscape is driven primarily by agricultural encroachment rather than urban development.

This vegetation-to-agriculture conversion pattern was closely associated with measurable structural fragmentation captured by the landscape metrics. As summarised in Table 1 and illustrated in Figure 8, the forest class exhibited a steady decline in *PLAND* and *LPI*, accompanied by increases in *ED* and *NP*, reflecting intensified boundary exposure and the loss of large contiguous forest cores. Conversely, agricultural classes showed concurrent increases in *PLAND* and *NP*, confirming their expansion into previously forested and shrub-dominated areas. Shrubland consistently decreased across all metrics, emphasising its role as the transitional class that is most affected by conversion. Built-up areas, although only slightly increasing in total extent, displayed a sharp rise in *NP*, indicating the emergence of dispersed urban clusters and the onset of peri-urban sprawl along the accessibility corridors. Collectively, these combined shifts doubled *NP* for dryland agriculture (from 295 in 2012 to 552 in 2036), while the landscape *LPI* dropped sharply (from 54.93 to 50.48), indicating a transition towards a more fragmented and spatially heterogeneous landscape. In contrast, *SHDI* increased (from 1.241 to 1.323), signifying increased compositional diversity but decreased ecological cohesion. These results align with regional findings across tropical Southeast Asia, where agricultural intensification has emerged as the dominant

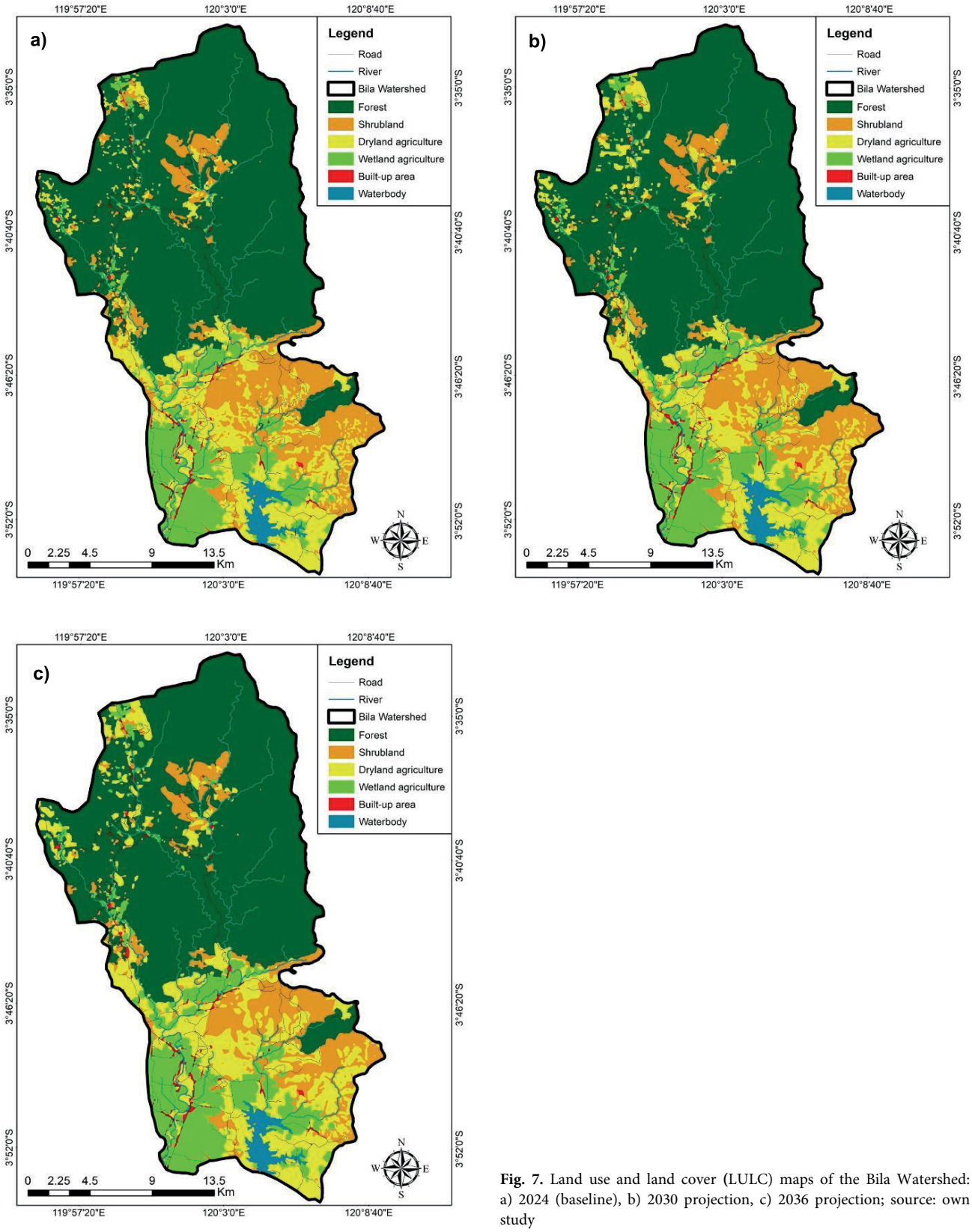

Fig. 7. Land use and land cover (LULC) maps of the Bila Watershed: a) 2024 (baseline), b) 2030 projection, c) 2036 projection; source: own study

mechanism of fragmentation (Santoro *et al.*, 2023; Zheng *et al.*, 2021). Comparable fragmentation trajectories have been documented in other Southeast Asian watersheds, where agricultural expansion has substantially increased patchiness and landscape division (Ma *et al.*, 2023). The decline in the Bila Watershed's *LPI* to about 50% is ecologically significant, as evidence shows biodiversity and connectivity thresholds often occur in the 30–50% forest cover range, beyond which hydrological connectivity and species persistence decline sharply (Shennan-Farpón *et al.*, 2021; Wies *et al.*, 2021).

Spatially, the upper watershed showed the highest fragmentation, aligning with the boundary between forest

Table 1. Summary of landscape metrics across land use and land cover (LULC) types in 2012, 2024, and 2036 for the Bila Watershed

LULC type	Metrics value in year														
	2012					2024					2036				
	PLAND	*NP*	*LPI*	*ED*	*SHDI*	*PLAND*	*NP*	*LPI*	*ED*	*SHDI*	*PLAND*	*NP*	*LPI*	*ED*	*SHDI*
Forest	0.56	55	54.935	0.0012	1.241	0.54	53	53.493	0.0016	1.285	0.51	50	50.485	0.0017	1.323
Shrubland	0.19	359	11.136	0.0023		0.16	425	8.300	0.0027		0.14	519	8.080	0.0029	
Agricultural dryland	0.14	295	3.163	0.0019		0.17	525	3.389	0.0027		0.19	552	3.491	0.0033	
Agricultural wetland	0.09	249	2.287	0.0006		0.11	329	3.255	0.0010		0.14	348	3.265	0.0011	
Built-up area	0.01	234	0.078	0.0003		0.01	378	0.100	0.0004		0.01	380	0.100	0.0005	
Waterbody	0.02	595	1.511	0.0007		0.02	596	1.511	0.0007		0.02	596	1.511	0.0007	
Mean	0.17	297.83	12.185	0.001	1.241	0.17	384.33	11.675	0.002	1.285	0.17	407.5	11.155	0.002	1.323

Explanations: *PLAND* = proportion of landscape, *NP* = number of patches, *LPI* = largest patch index, *ED* = edge density, and *SHDI* = Shannon's diversity index.
Source: own study.

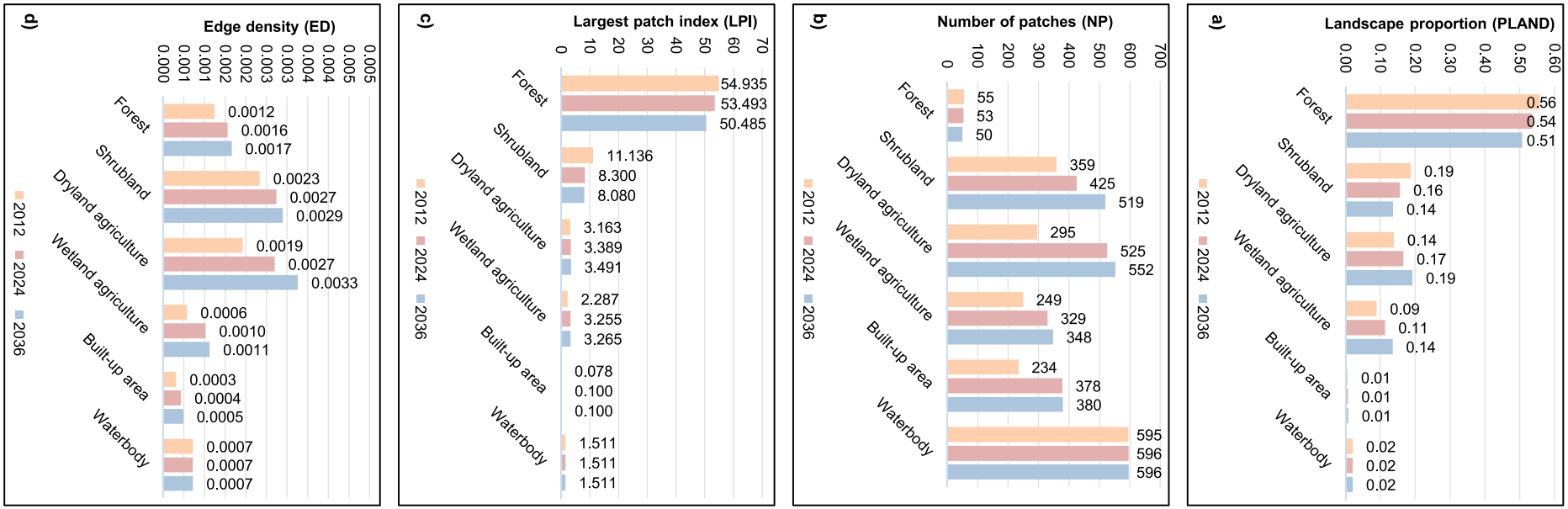

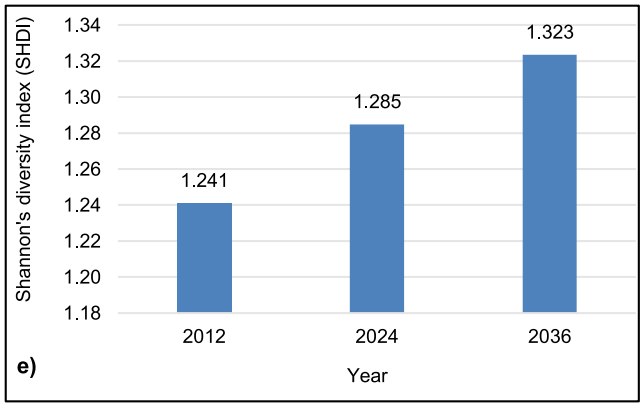

Fig. 8. Landscape metrics in the Bila Watershed from 2012 to 2036, including: a) proportion of landscape (*PLAND*), b) number of patches (*NP*), c) largest patch index (*LPI*), d) edge density (ED), e) Shannon's diversity index (*SHDI*); source: own study

contraction and agricultural diffusion. If left unmanaged, these transitions may exacerbate slope instability, reduce infiltration capacity, and increase sediment loading in the Lake Tempe, patterns that have been widely documented in fragmented tropical uplands (Liu *et al.*, 2022; Patil *et al.*, 2023). Moreover, the observed increase in patch density without a corresponding increase in vegetation recovery indicates that the system is undergoing functional fragmentation rather than cyclical regeneration. This implies a potential loss of ecological resilience and disruption of ecosystem services, such as carbon storage, microclimatic regulation, and surface runoff moderation (Ellis and Eaton, 2021; Hisano *et al.*, 2024).

In policy terms, these findings highlight the urgency of implementing spatially coordinated land-use zoning and agroforestry buffer systems in upper watersheds. Integrating ecological thresholds, such as maintaining the *LPI* above 50% and limiting *ED* growth below 0.003 m·ha^{-1}, could serve as practical benchmarks for regional planning, consistent with recent ecological threshold modelling in tropical catchments (Wies *et al.*, 2021; Zhang *et al.*, 2021). Overall, these results emphasise that fragmentation in the Bila Watershed is not merely a matter of LULC conversion, but a spatial restructuring process that directly influences watershed function and sustainability.

Although formal statistical testing was not conducted due to the limited time intervals, the observed monotonic changes in *NP*, *LPI*, and *ED* showed consistent directional trends that are ecologically important and aligned with the fragmentation dynamics reported in recent studies (Jato-Espino and Lierow, 2024; Kerr and Remmel, 2024). The strong directional coherence across metrics indicates that the changes are not random fluctuations, but systematic spatial transformations driven by LULC pressure. Uncertainties persist due to the 30 m spatial resolution, misclassification in mixed-cover zones, and the business-as-usual scenario excluding socioeconomic interventions. Despite these limitations, the use of open-source data, validated ANN modelling, and reproducible GIS workflows ensures that the trends reported here represent a reliable approximation of real-world processes and a transparent foundation for future scenario-based or policy-integrated modelling.

CONCLUSIONS

This study demonstrates a methodological advancement in landscape modelling by integrating cellular automata–artificial neural network (CA–ANN) simulation and landscape metrics within a single, reproducible GIS framework (QGIS 3.34). This hybrid method allows for predicting land-use change and understanding its structure, expanding CA–ANN models beyond spatial accuracy alone to analyse fragmentation in tropical watersheds. The proposed framework enhances methodological transparency, supports reproducible research practices, and provides a practical basis for evidence-based spatial planning and sustainable watershed management.

The empirical application of this framework to the Bila Watershed revealed significant land-use transitions and fragmentation dynamics from 2012 to 2036. During this period, forest cover declined by 2,781.13 ha (−9.14%), whereas dryland and wetland agriculture expanded by 2,914.39 ha (38.52%) and 2,520.76 ha (51.88%), respectively. These transitions were accompanied by increased fragmentation, as reflected by a decline in the largest patch index (from 54.93 to 50.48), a near doubling of the number of patches for dryland agriculture (from 295 to 552), and a 74% increase in edge density for dryland agriculture. The model achieved high predictive reliability ($k_{overall}$ = 0.94; *OA* = 96.19%), thereby validating its effectiveness in simulating complex land transitions. Besides, Shannon's diversity index increased from 1.241 to 1.323, indicating heightened landscape heterogeneity and spatial disorder in the area.

By shifting from purely spatial projection to structural interpretation, this hybrid framework enhances the ecological and policy relevance of Land Use and Land Cover (LULC) simulations. It allows model outputs to be interpreted in terms of landscape structure and ecological function, thereby strengthening the link between science and policy. This facilitates identification of fragmentation hotspots, informs climate-resilient land management strategies, and supports spatial planning aligned with Sustainable Development Goal 15, particularly in ecologically sensitive upstream zones of the watershed.

These findings emphasise the importance of integrating structural metrics into future land-use models to ensure sustainability in the face of accelerating anthropogenic pressures. However, this study is limited by the spatial data resolution and the exclusion of complex socioeconomic drivers that can influence LULC dynamics in tropical regions. Future research should incorporate higher-resolution datasets and agent-based models to capture the influence of human behaviour on landscape dynamics more comprehensively.

ABBREVIATIONS

ANN = artificial neural network
CA = cellular automata
ED = edge density
LecoS = landscape ecology statistics
LPI = largest patch index
LULC = land use and land cover
MOLUSCE = modules for land use change evaluation
NP = number of patches

PLAND = proportion of landscape
QGIS = quantum geographic information system
SHDI = Shannon's diversity index

ACKNOWLEDGMENTS

The authors would like to express their sincere appreciation to the Center for Higher Education Funding and Assessment (PPAPT), the Indonesia Endowment Fund for Education (LPDP), the Indonesian Education Scholarship (BPI), and Hasanuddin University for their academic and institutional support throughout the completion of this research and the preparation of this article.

FUNDING

This research was conducted as part of a doctoral programme funded under contract number 011469/PPAPT.1.2/BPI.06/02/2025 by the Center for Higher Education Funding and Assessment (PPAPT) through the Indonesia Endowment Fund for Education (LPDP), under the Indonesian Education Scholarship (BPI) programme.

CONFLICT OF INTERESTS

All authors declare that they have no conflicts of interests.

INSTITUTIONAL REVIEW BOARD STATEMENT

This study did not involve animals or plants requiring ethical approval.

REFERENCES

Abbas, Z. *et al.* (2021) "Spatiotemporal change analysis and future scenario of LULC using the CA-ANN Approach: A case study of the Greater Bay Area, China," *Land,* 10(6), pp. 584. Available at: https://doi.org/10.3390/LAND10060584.

Abdullah, A. *et al.* (2022) "Proyeksi Kerawanan Banjir pada Lahan Sawah Berbasis Model Iklim HadCM3 di DAS Bila Provinsi Sulawesi Selatan [Flood vulnerability projection in rice land based on the HadCM3 climate model in the Bila Watershed Province of South Sulawesi]," *Jurnal Galung Tropika*, 11(2), pp. 143–152. Available at: https://doi.org/10.31850/jgt.v11i2.898.

Adıyaman, H. *et al.* (2025) "Stripe error correction for Landsat-7 using deep learning," *PFG – Journal of Photogrammetry, Remote Sensing and Geoinformation Science*, 93(1), pp. 51–63. Available at: https://doi.org/10.1007/S41064-024-00306-X.

Alaei, N. *et al.* (2022) "Spatial comparative analysis of landscape fragmentation metrics in a watershed with diverse land uses in Iran," *Sustainability*, 14, 14876. Available at: https://doi.org/10.3390/SU142214876.

Alemayehu, B., Suarez-Minguez, J. and Rosette, J. (2024) "The implications of plantation forest-driven land use/land cover changes for ecosystem service values in the Northwestern Highlands of Ethiopia," *Remote Sensing*, 16(22), pp. 4159. Available at: https://doi.org/10.3390/RS16224159.

Asra, R., Mappiasse, M.F. and Nurnawati, A.A. (2020) "The application of CA-Markov model for prediction of land use change in Sub-Watershed Bila Year 2036," *AGROVITAL : Jurnal Ilmu Pertanian*, 5(1), pp. 1–10. Available at: https://doi.org/10.35329/agrovital.v5i1.630.

Baig, M.F. *et al.* (2022) "Assessment of land use land cover changes and future predictions using CA-ANN simulation for Selangor, Malaysia," *Water*, 14(3), 402. Available at: https://doi.org/10.3390/W14030402.

Belay, H., Melesse, A.M. and Tegegne, G. (2024) "Scenario-based land use and land cover change detection and prediction using the cellular automata–Markov model in the Gumara Watershed, Upper Blue Nile Basin, Ethiopia," *Land*, 13(3), 396. Available at: https://doi.org/10.3390/land13030396.

Biswas, J. *et al.* (2023) "Mapping and monitoring land use land cover dynamics employing Google Earth Engine and machine learning algorithms on Chattogram, Bangladesh," *Heliyon*, 9(11). Available at: https://doi.org/10.1016/j.heliyon.2023.e21245.

Blissag, B., Yebdri, D. and Kessar, C. (2024) "Spatiotemporal change analysis of LULC using remote sensing and CA-ANN approach in the Hodna basin, NE of Algeria," *Physics and Chemistry of the Earth, Parts A/B/C*, 133, 103535. Available at: https://doi.org/10.1016/J.PCE.2023.103535.

BSN (2010) *Klasifikasi penutup lahan - Bagian 1: Skala kecil dan menengah [National Land Cover Classification Based on SNI 7645:2010].* Badan Standardisasi Nasional. Available at: https://big.go.id/assets/download/sni/SNI/15.%20SNI%207645-2010%20Klasifikasi%20penutup%20lahan.pdf (Accessed: June 30, 2025).

BSN (2014) *National Land Cover Classification Based on SNI 7645:2014.* Badan Standardisasi Nasional. Available at: https://kupdf.net/download/sni-7645-1-2014-klasifikasi-penutup-lahan_59edda7908bbc53933eb8a1f_pdf (Accessed: June 30, 2025).

Cabernard, L., Pfister, S. and Hellweg, S. (2024) "Biodiversity impacts of recent land-use change driven by increases in agri-food imports," *Nature Sustainability*, 7(11), pp. 1512–1524. Available at: https://doi.org/10.1038/s41893-024-01433-4.

Christiawan, P.I. and Nguyen, T.P.L. (2024) "Peri-urbanization in populous developing Asian countries: A systematic review," *International Journal of Sustainable Development and Planning*, 19(3), 949. Available at: https://doi.org/10.18280/IJSDP.190313.

Congedo, L. (2021) "Semi-automatic classification plugin: A Python tool for the download and processing of remote sensing images in QGIS," *Journal of Open Source Software*, 6(64), 3172. Available at: https://doi.org/10.21105/joss.03172.

Dharmawan, I.W.S. *et al.* (2023) "Implementation of soil and water conservation in Indonesia and its impacts on biodiversity, hydrology, soil erosion and microclimate," *Applied Sciences*, 13(13), 7648. Available at: https://doi.org/10.3390/APP13137648.

Diep, H. *et al.* (2025) "Benefits and trade-offs from land use and land cover changes under different scenarios in the coastal delta of Vietnam," *Land*, 14(5), 1063. Available at: https://doi.org/10.3390/LAND14051063.

Din, S.U. and Yamamoto, K. (2024) "Urban spatial dynamics and geo-informatics prediction of Karachi from 1990–2050 using remote sensing and CA-ANN simulation," *Earth Systems and Environment*, 8(3), pp. 849–868. Available at: https://doi.org/10.1007/S41748-024-00439-4.

El Moussaoui, E.H. *et al.* (2025) "A comparative methodological approach for argan forest classification using Landsat imagery," *Environmental Monitoring and Assessment*, 197(2), 210. Available at: https://doi.org/10.1007/S10661-025-13649-8.

Ellis, C.J. and Eaton, S. (2021) "Microclimates hold the key to spatial forest planning under climate change: Cyanolichens in temperate

rainforest," *Global Change Biology*, 27(9), pp. 1915–1926. Available at: https://doi.org/10.1111/GCB.15514.

FAO (2020) *Global forest resources assessment 2020. Main report*. 1st edn. Rome: Food and Agriculture Organization of the United Nations. Available at: https://doi.org/10.4060/ca9825en.

Fetene, D.T., Lohani, T.K. and Mohammed, A.K. (2023) "LULC change detection using support vector machines and cellular automata-based ANN models in Guna Tana watershed of Abay basin, Ethiopia," *Environmental Monitoring and Assessment*, 195(11), pp. 1–17. Available at: https://doi.org/10.1007/S10661-023-11968-2.

García-Álvarez, D. and Paegelow, M. (2022) "Spatial metrics to validate land use cover maps," in D. García-Álvarez *et al.* (eds.) *Land use cover datasets and validation tools: Validation practices with QGIS*. Cham: Springer, pp. 205–228. Available at: https://doi.org/10.1007/978-3-030-90998-7_11.

Gharaibeh, A. *et al.* (2020) "Improving land-use change modeling by integrating ANN with cellular automata-Markov chain model," *Heliyon*, 6(9). Available at: https://doi.org/10.1016/j.heliyon.2020.e05092.

Gong, J. *et al.* (2023) "Simulation and prediction of land use in urban agglomerations based on the PLUS model: A case study of the Pearl River Delta, China," *Frontiers in Environmental Science*, 11, 1306187. Available at: https://doi.org/10.3389/FENVS.2023.1306187.

Hansen, M.C. *et al.* (2020) "The fate of tropical forest fragments," *Science Advances*, 6(11), pp. 8574–8585. Available at: https://doi.org/10.1126/SCIADV.AAX8574.

Harrison, M.E. *et al.* (2019) "Tropical forest and peatland conservation in Indonesia: Challenges and directions," *People and Nature*, 2(1), pp. 4–28. Available at: https://doi.org/10.1002/PAN3.10060.

Hisano, M. *et al.* (2024) "Functional diversity enhances dryland forest productivity under long-term climate change," *Science Advances*, 10(17), 4152. Available at: https://doi.org/10.1126/SCIADV.ADN4152.

Huang, Y. *et al.* (2024) "An integrated framework for landscape indices' calculation with raster–vector integration and its application based on QGIS," *ISPRS International Journal of Geo-Information*, 13(7), 242. Available at: https://doi.org/10.3390/IJGI13070242.

Hussain, K. *et al.* (2025) "Analysing LULC transformations using remote sensing data: insights from a multilayer perceptron neural network approach," *Annals of GIS*, 31(3), pp. 473–500. Available at: https://doi.org/10.1080/19475683.2024.2343399.

Islam, M.Y. *et al.* (2023) "Quantifying forest land-use changes using remote-sensing and CA-ANN model of Madhupur Sal Forests, Bangladesh," *Heliyon*, 9(5), 15617. Available at: https://doi.org/10.1016/J.HELIYON.2023.E15617.

Jato-Espino, D. and Lierow, S. (2024) "Spatiotemporal analysis of landscape dynamics and their use as input for the design of a habitat suitability index: A case study of *Oryctolagus cuniculus* in a Mediterranean region," *Ecological Informatics*, 82, 102731. Available at: https://doi.org/10.1016/J.ECOINF.2024.102731.

Kamaraj, M. and Rangarajan, S. (2022) "Predicting the future land use and land cover changes for Bhavani basin, Tamil Nadu, India, using QGIS MOLUSCE plugin," *Environmental Science and Pollution Research*, 29(57), pp. 86337–86348. Available at: https://doi.org/10.1007/S11356-021-17904-6.

Kerr, B. and Remmel, T.K. (2024) "Activity-based measures of landscape fragmentation," *Landscape Ecology*, 39(12), pp. 1–18. Available at: https://doi.org/10.1007/S10980-024-01987-W.

Leta, M.K., Demissie, T.A. and Tränckner, J. (2021) "Hydrological responses of watershed to historical and future land use land cover change dynamics of Nashe Watershed, Ethiopia," *Water*, 13(17), 2372. Available at: https://doi.org/10.3390/W13172372.

Li, J. *et al.* (2025) "Effects of pattern dynamics on carbon storage capacity in the Qinghai-Tibetan Plateau from 1980 to 2020," *Scientific Reports*, 15(1), pp. 1–18. Available at: https://doi.org/10.1038/S41598-025-07392-W.

Liang, X. *et al.* (2021) "Understanding the drivers of sustainable land expansion using a patch-generating land use simulation (PLUS) model: A case study in Wuhan, China," *Computers, Environment and Urban Systems*, 85, 101569. Available at: https://doi.org/10.1016/J.COMPENVURBSYS.2020.101569.

Lin, M. *et al.* (2024) "Scale and zoning effects on landscape metrics for assessing ecological stress from urban expansion," *Landscape Ecology*, 39(12), pp. 1–16. Available at: https://doi.org/10.1007/S10980-024-02012-W.

Liu, Y. *et al.* (2022) "Assessment of spatial-temporal changes of landscape ecological risk in Xishuangbanna, China from 1990 to 2019," *Sustainability*, 14(17), 10645. Available at: https://doi.org/10.3390/SU141710645.

Lukas, P., Melesse, A.M. and Kenea, T.T. (2023) "Prediction of future land use/land cover changes using a coupled CA-ANN model in the Upper Omo–Gibe River Basin, Ethiopia," *Remote Sensing*, 15(4). Available at: https://doi.org/10.3390/RS15041148.

Ma, S. *et al.* (2023) "Direct and indirect effects of agricultural expansion and landscape fragmentation processes on natural habitats," *Agriculture, Ecosystems & Environment*, 353, 108555. Available at: https://doi.org/10.1016/J.AGEE.2023.108555.

Maity, N. and Mishra, V.N. (2024) "Urban growth analysis using multi-temporal remote sensing image and landscape metrics for smart city planning of Lucknow District, India," *Engineering Proceedings*, 82(1), 59. Available at: https://doi.org/10.3390/ECSA-11-20514.

Mancino, G. *et al.* (2020) "Cross-comparison between Landsat 8 (OLI) and Landsat 7 (ETM+) derived vegetation indices in a Mediterranean environment," *Remote Sensing*, 12(2), 291. Available at: https://doi.org/10.3390/RS12020291.

Matyukira, C. and Mhangara, P. (2023) "Land cover and landscape structural changes using extreme gradient boosting random forest and fragmentation analysis," *Remote Sensing*, 15(23), 5520. Available at: https://doi.org/10.3390/RS15235520.

Mendoza-Ponce, A. *et al.* (2021) "Impacts of land management and climate change in a developing and socioenvironmental challenging transboundary region," *Journal of Environmental Management*, 300, 113748. Available at: https://doi.org/10.1016/J.JENVMAN.2021.113748.

Mishra, O. *et al.* (2024) *Prediction of land use land cover change using a coupled CA-ANN modeling in Dhanusha district of Nepal*. Available at: https://doi.org/10.21203/RS.3.RS-5301403/V1.

Moreira, R.M. *et al.* (2024) "A landscape ecology approach: Modeling forest fragmentation with artificial neural networks and cellular-automata Markov-chain for improved environmental policy in the southwestern Brazilian Amazon," *Land Degradation and Development*, 35(2), pp. 687–704. Available at: https://doi.org/10.1002/LDR.4945.

Muhammad, R. *et al.* (2022) "Spatiotemporal change analysis and prediction of future land use and land cover changes using QGIS MOLUSCE plugin and remote sensing big data: A case study of Linyi, China," *Land*, 11(3), 419. Available at: https://doi.org/10.3390/LAND11030419.

Pandey, S., Kumari, N. and Al Nawajish, S. (2023) "Land use land cover (LULC) and surface water quality assessment in and around selected dams of Jharkhand using water quality index (WQI) and Geographic Information System (GIS)," *Journal of the Geological*

Society of India, 99(2), pp. 205–218. Available at: https://doi.org/10.1007/S12594-023-2288-Y.

Patil, M. *et al.* (2023) "Identification of potential zones on the estimation of direct runoff and soil erosion for an ungauged watershed based on remote sensing and GIS techniques," *International Journal of Engineering and Geosciences*, 8(3), pp. 224–238. Available at: https://doi.org/10.26833/IJEG.1115608.

Perez, M. and Vitale, M. (2023) "Landsat-7 ETM+, Landsat-8 OLI, and Sentinel-2 MSI surface reflectance cross-comparison and harmonization over the Mediterranean basin area," *Remote Sensing*, 15(16), 4008. Available at: https://doi.org/10.3390/RS15164008.

Putra, A.N. *et al.* (2025) "Potential erosion and sedimentation based on land use change by using cellular automata-artificial neural network," *Geomatics, Natural Hazards and Risk*, 16(1), 2461058. Available at: https://doi.org/10.1080/19475705.2025.2461058.

Rojas Celis, A.P., Shen, J. and Martinez Otalora, J.D. (2025) "Spatiotemporal land use and land cover changes and their impact on landscape patterns in the Colombian Coffee Cultural Landscape (2014–2034)," *Land*, 14(5), 1045. Available at: https://doi.org/10.3390/LAND14051045.

Santoro, A., Piras, F. and Yu, Q. (2023) "Spatial analysis of deforestation in Indonesia in the period 1950–2017 and the role of protected areas," *Biodiversity and Conservation*, pp. 1–27. Available at: https://doi.org/10.1007/S10531-023-02679-8.

Sharma, A. K. *et al.* (2022) "Assessment of land use change and climate change impact on biodiversity and environment," *Springer Proceedings in Earth and Environmental Sciences*, pp. 73–89. Available at: https://doi.org/10.1007/978-3-031-05335-1_5.

Shennan-Farpón, Y., Visconti, P. and Norris, K. (2021) "Detecting ecological thresholds for biodiversity in tropical forests: Knowledge gaps and future directions," *Biotropica*, 53(5), pp. 1276–1289. Available at: https://doi.org/10.1111/BTP.12999.

Sujarwo, M.W., Hakim, F.L. and Indarto, I. (2023) "Using Landsat to track land use and land cover (LULC) change from 1970 to 2020 in Mayang watershed, East Jawa," in P. Zhang and T.A. Siswoyo (eds.) *The 5th International Conference on Agriculture and Life Science 2021 (ICALS 2021): "Accelerating transformation in industrial agriculture through sciences implementation"* 3–4 November 2021 Jember, Indonesia. *AIP Conference Proceedings*, 2583(1), 060002. Available at: https://doi.org/10.1063/5.0117111.

Talukdar, S. *et al.* (2021) "Modeling fragmentation probability of land-use and land-cover using the bagging, random forest and random subspace in the Teesta River Basin, Bangladesh," *Ecological Indicators*, 126, 107612. Available at: https://doi.org/10.1016/J.ECOLIND.2021.107612.

Thomas, A. *et al.* (2020) "Fragmentation and thresholds in hydrological flow-based ecosystem services," *Ecological Applications*, 30(2), e02046. Available at: https://doi.org/10.1002/EAP.2046.

Toosi, N.B. *et al.* (2020) "Land cover classification in mangrove ecosystems based on VHR satellite data and machine learning – An upscaling approach," *Remote Sensing*, 12(17), 2684. Available at: https://doi.org/10.3390/RS12172684.

Uddin, M.S., Mahalder, B. and Mahalder, D. (2023) "Assessment of land use land cover changes and future predictions using CA-ANN simulation for Gazipur City corporation, Bangladesh," *Sustainability*, 15(16), 12329. Available at: https://doi.org/10.3390/SU151612329.

Wies, G., Nicasio Arzeta, S. and Martinez Ramos, M. (2021) "Critical ecological thresholds for conservation of tropical rainforest in human modified landscapes," *Biological Conservation*, 255, 109023. Available at: https://doi.org/10.1016/J.BIOCON.2021.109023.

Xu, Q. *et al.* (2021) "Simulation of land-use changes using the partitioned ANN-CA model and considering the influence of land-use change frequency," *ISPRS International Journal of Geo-Information*, 10(5), 346. Available at: https://doi.org/10.3390/IJGI10050346.

Zhang, T. *et al.* (2025) "Analyzing cropland fragmentation evolution and driving mechanisms in Shandong through MSPA and landscape metrics integration," *Scientific Reports*, 15(1), pp. 1–21. Available at: https://doi.org/10.1038/S41598-025-05964-4.

Zhang, X. *et al.* (2021) "Water quality variability affected by landscape patterns and the associated temporal observation scales in the rapidly urbanizing watershed," *Journal of Environmental Management*, 298, 113523. Available at: https://doi.org/https://doi.org/10.1016/j.jenvman.2021.113523.

Zheng, Z. *et al.* (2021) "Anthropogenic impacts on late holocene land-cover change and floristic biodiversity loss in tropical southeastern Asia," *Proceedings of the National Academy of Sciences*, 118(40), e2022210118. Available at: https://doi.org/10.1073/PNAS.2022210118.

Zhu, Z. *et al.* (2021) "Analysis of the spatiotemporal changes in watershed landscape pattern and its influencing factors in rapidly urbanizing areas using satellite data," *Remote Sensing*, 13(6), 1168. Available at: https://doi.org/10.3390/RS13061168.